Purdue University Purdue e-Pubs

Birck and NCN Publications

Birck Nanotechnology Center

1-2008

Quantitative evaluation of covalently bound molecules on GaP (100) surfaces

Rosangelly Flores-Perez Purdue University - Main Campus, rflores@purdue.edu

Dmitry Zemlyanov Birck Nanotechnology Center, Purdue University, dimazemlyanov@purdue.edu

Albena Ivanisevic Purdue University - Main Campus, albena@purdue.edu

Follow this and additional works at: http://docs.lib.purdue.edu/nanopub



Part of the Nanoscience and Nanotechnology Commons

Flores-Perez, Rosangelly; Zemlyanov, Dmitry; and Ivanisevic, Albena, "Quantitative evaluation of covalently bound molecules on GaP (100) surfaces" (2008). Birck and NCN Publications. Paper 327. http://docs.lib.purdue.edu/nanopub/327

This document has been made available through Purdue e-Pubs, a service of the Purdue University Libraries. Please contact epubs@purdue.edu for additional information.



Subscriber access provided by Purdue University Libraries

Article

Quantitative Evaluation of Covalently Bound Molecules on GaP (100) Surfaces

Rosangelly Flores-Perez, Dmitry Y. Zemlyanov, and Albena Ivanisevic

J. Phys. Chem. C, 2008, 112 (6), 2147-2155• DOI: 10.1021/jp710437v • Publication Date (Web): 19 January 2008

Downloaded from http://pubs.acs.org on February 16, 2009

More About This Article

Additional resources and features associated with this article are available within the HTML version:

- Supporting Information
- Links to the 1 articles that cite this article, as of the time of this article download
- · Access to high resolution figures
- Links to articles and content related to this article
- Copyright permission to reproduce figures and/or text from this article

View the Full Text HTML



Quantitative Evaluation of Covalently Bound Molecules on GaP (100) Surfaces

Rosangelly Flores-Perez,† Dmitry Y. Zemlyanov,‡ and Albena Ivanisevic*,†,§

Department of Chemistry, Birck Nanotechnology Center, Weldon School of Biomedical Engineering, Purdue University, West Lafayette, Indiana 47907

Received: October 29, 2007; In Final Form: November 16, 2007

The study utilizes surface sensitive techniques in order to quantitatively characterize the nature of organization and bonding of alkanethiol adsorbates on GaP (100) surfaces. The evaluation was performed using water contact angle, atomic force microscopy (AFM), Fourier transform infrared (FT-IR) spectroscopy, and X-ray photoelectron spectroscopy (XPS). The hydrophobicity and consistency of surface roughness were studied via water contact angle and AFM. The FT-IR experimental protocol permitted the identification of characteristic functional groups on the surface and enabled insight into the organization within the adlayers on the GaP surface. XPS data showed evidence for the formation of a covalent bond between the sulfur and the surface and was used to calculate the adlayer thicknesses, tilt angles, and molecular coverages for different adsorbates. The thickness and tilt angles values were comparable to other modified semiconductor materials. High coverages were observed for all alkanethiols on GaP (100). The quantitative XPS protocol reported can be applied to the evaluation of other adsorbates on semiconductor materials.

1. Introduction

The ability to control the formation of molecular layers on III-V semiconductor surfaces can eventually result in industrially applicable passivation strategies. 1-6 Longer surface stability can be achieved if one directly attaches protective organic moieties to the chalcogenide atoms. The success of this straight forward functionalization route depends on the removal of the native oxide layer that forms on III-V surfaces. 7,8 The formation of covalent bonds with surface atoms, low tilt angles of the anchored molecules, and high surface coverages are desired characteristics for hybrid organic-inorganic interfaces based on semiconductor materials. In recent years comprehensive and quantitative surface studies of SAMs on GaAs have been published.⁹ Such studies have allowed researchers to understand what kind of control can be established over specific desired characteristics. However, relatively few reports have dealt with the quantitative characterization of covalently bound molecules to other types of III-V materials.⁵

Gallium phosphide (GaP) is a commonly used III—V semiconductor material especially in light emitting⁴ and high-temperature devices. GaP subtrates have a low thermal regeneration rate which means that they can be utilized in charge storage devices with extensive retention time. ¹⁰ In addition, this material has been shown to possess strong photocorrosion resistance¹¹ and has been incorporated in useful low-noise detection photodiodes at low cost. ¹² The rapid formation of thermal oxide layer on the GaP leads to difficulties in adapting this material to sensing platforms despite its other useful properties. A relatively small number of research groups^{4,13} have studied the molecular passivation of GaP as a way to prevent oxide reformation on the surface. If this strategy is successful, the degradation of the material can be prevented. Furthermore,

TABLE 1: Summary of the Initial Characterization of Clean GaP(100) and Modified GaP(100) with ODT, MHA, MUAM, and MHL

surface	water contact angle (°)	roughness (nm)
1. clean GaP	19 ± 1	0.190 ± 0.02
2. ODT	103 ± 3	0.471 ± 0.04
3. MHA	66 ± 3	0.535 ± 0.08
4. MUAM	79 ± 1	0.557 ± 0.03
5. MHL	38 ± 2	0.505 ± 0.03

if chemically reactive groups are available on the surface after the surface passivation, one can built functional and stable assemblies on this III—V semiconductor material using covalent or electrostatic interactions.

In this paper we study the formation of adlayers on GaP (100). The adsorbates studied were octadecanethiol (ODT), 16mercatohexadecanoic acid (MHA), 11-amino-1-undecanethiol hydrochloride (MUAM), and mercapto-1-hexanol (MHL). A number of characterization techniques, water contact angle, atomic force microscopy (AFM), Fourier transform infrared (FT-IR), and X-ray photoelectron spectroscopy (XPS), were used to understand the coverage, nature of bonding, tilt angle and stability of the adlayers. The quantitative data we present allowed us to understand the nature of the sulfur-substrate bond. In addition, we calculated the adlayer thickness after each adsorbate was used to functionalize the surface. The thickness values extracted from XPS measurements were in agreement with the AFM observations. In the case of all adsorbates, we observed very high coverages on GaP (100). The study also discusses some notable differences among the tilt angles of short vs long alkanethiol molecules.

2. Experimental Section

2.1. Reagents and Materials. Double-polished S-doped *n*-type gallium phosphide (GaP [100]) wafers were purchased from University Wafer (South Boston, MA). 1-Octadecanethiol (ODT, 98%), 16-mercatohexadecanoic acid (MHA, 90%), and

^{*} Corresponding author. Tel.: 765-496-3676. Fax: 765-494-1193. E-mail: albena@purdue.edu.

[†] Department of Chemistry.

[‡] Birck Nanotechnology Center.

[§] Weldon School of Biomedical Engineering.

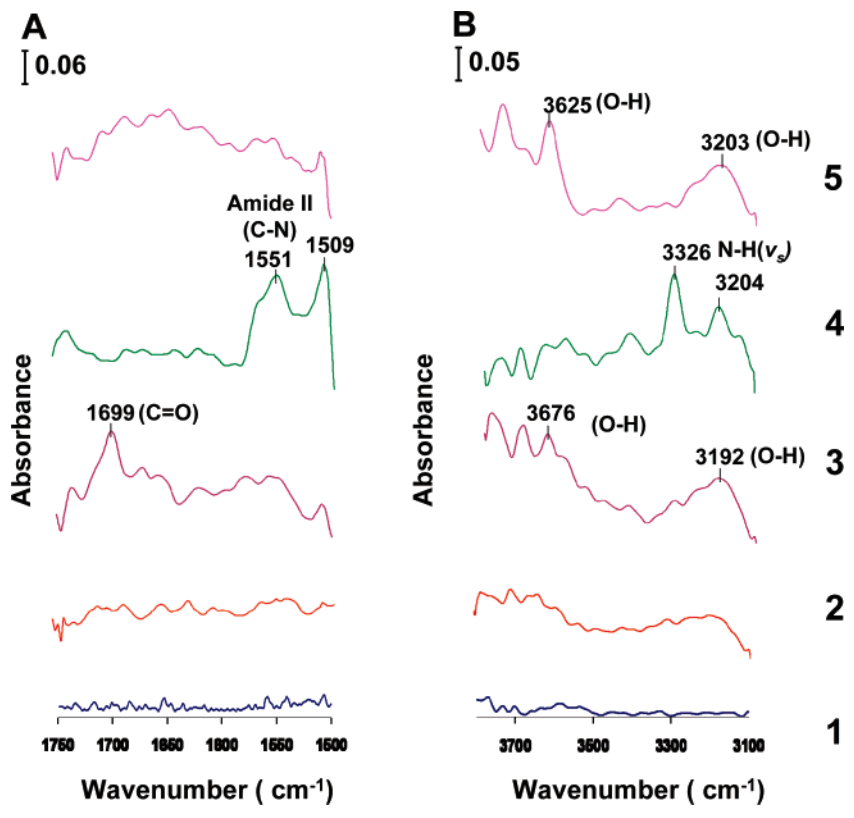


Figure 1. FTIR spectra of (A) the region between 1750 and 1500 cm⁻¹ and (B) the region between 3800 and 3100 cm⁻¹. The following samples are presented: (1) clean GaP(100), (2) ODT/GaP(100), (3) MHA/GaP(100), (4) MUAM/GaP(100), and (5) MHL/GaP(100).

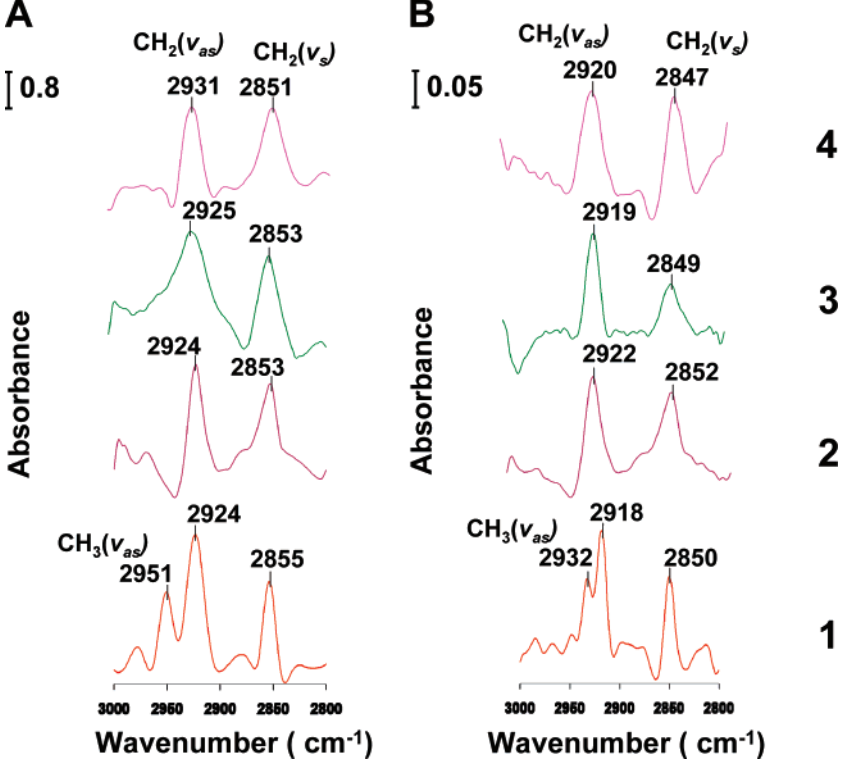


Figure 2. FTIR data for the region between 3000 and 2800 cm⁻¹ collected (A) in ethanol solution and (B) on GaP (100). Data for the following adsorbates is shonw: (1) ODT, (2) MHA, (3) MUAM, and (4) MHL.

mercapto-1-hexanol (MHL, 97%) were obtained from Sigma-Aldrich. 11-Amino-1-undecanethiol hydrochloride (MUAM, 90%) was acquired from Dojindo Laboratories.

2.2. Surface Cleaning and Functionalization. Each n-type GaP:S wafer was cut into 1×1 cm² pieces which were sonicated in pure water, ethanol, and methanol for 10 min and

subsequently dried with nitrogen gas (N₂). Each surface was cleaned in aqua regia solution^{14,15} (HCl (36%): HNO₃ (70%),3: 1/v:v) for 30 s at 40 °C. *Caution: Aqua regia solution is extremely hot!* After the cleaning treatment the surfaces were rinsed with water and dried with N₂. The samples were then incubated in ODT, MHA, MHL and MUAM ethanolic solutions

TABLE 2: Summary of the Peak Positions of Ga 3d, P 2p, S 2p/Ga 3s, S 2s, C 1s, and N 1s Obtained from Clean GaP(100) and Modified GaP(100) with ODT, MHA, MUAM, and MHL

	peak assignments	binding energy, eV				
		clean GaP(100)	ODT/ GaP(100)	MHA/ GaP(100)	MUAM/ GaP(100)	MHL/ GaP(100)
Ga 3d _{5/2}	GaP ^a	19.0	19.1	19.2	19.3	19.2
	Ga_2O_3	19.9	19.9	19.9	19.9	20.1
P 2p _{3/2}	GaP*	128.6	128.7	128.8	128.9	128.8
1	P_xO_y	133.5	133.5	133.5	133.6	133.7
S 2p _{3/2}	S* bound to Ga		162.2	162.6	162.8	162.3
•	S^a unbound				163.2	
	SO_x		168.9	168.7	168.5	169.0
Ga 3s	GaP	159.8	159.9	159.9	160.1	160.0
S 2s	S bound to Ga		226.7	227.1	227.2	227.2
	SO_x		234.8	233.8	232.1	232.9
C 1s	C-C	284.8	284.8	284.8	284.8	284.8
	C-OH	286.2				286.0
	O-C=O	287.0				
	HO-C=O			288.8		
	C-N				286.6	
N 1s	Ga 3d (Auger) L ₃ M ₄₅ M ₄₅	390.1, 392.3, 393.7, 395.3, 398.7	390.1, 392.3, 393.8, 395.3, 398.7	390.3, 392.5, 393.9, 395.4, 398.9	390.4, 392.6, 394.0, 395.4, 398.9	390.3, 392.5, 394.0, 395.5, 398.9
	NH ₂ /NH ₃ ⁺				399.5	

^a In the case of doublets such as Ga 3d_{5/2} and Ga 3d_{3/2}, P 2p_{3/2} and P 2p_{1/2}, and S 2p_{3/2} and S 2p_{1/2}, the peak position for the main component is provided due to the fact that the spin-orbital splitting was fixed during the curve-fitting.

(1 mM) for 24 h. Prior to any analysis each sample was washed with pure ethanol solvent several times and dried with N_2 gas.

2.3. Surface Characterization. *2.3.1. Water Contact Angle Measurements.* All water contact angle measurements were done on a Tantac, Inc. Contact Angle Meter, model CAM-PLUS. The half-angle method was utilized to determine the angles. At least five measurements were taken for each type of surface and then averaged.

2.3.2. Atomic Force Microscopy (AFM). Tapping mode AFM images were collected using a Multi-Mode Nanoscope IIIa Atomic Force Microscope. Single beam cantilevers were purchased from Veeco Instruments, CA, model # OTESPA7. They had a spring constant of 12-103 N/m. Each sample was evaluated using a scan size of $1\times1~\mu\mathrm{m}^2$ and scan rate of 1.5-2 Hz. Images were processed using the Nanoscope III 5.12r3 software. The average roughness of each sample was calculated using the data from 5 images collected on a given surface.

2.3.3. Fourier Transform IR (FT-IR) Spectroscopy. We utilized a Thermo Nicolet, Nexus 670 FT-IR spectrometer for all FT-IR experiments. This transmission mode instrument was coupled to an IR source and DTGS KBr detector. The spectrometer was purged with N₂ gas to remove any amount of water in the sample compartment prior to any data collection. The data were analyzed with the Thermo Nicolet's OMNIC software. Each data set was acquired with a resolution of 4 cm⁻¹. A background spectrum in N₂ atmosphere was always collected for each region of interest and subsequently subtracted from the sample spectra. Three different regions were examined: 1550–1800, 2800–3000, and 3100–3800 cm⁻¹.

2.3.4. X-ray Photoelectron Spectroscopy (XPS). XPS data were obtained with a Kratos Ultra DLD spectrometer using monochromatic Al K α radiation ($h\nu=1486.58$ eV). The survey and high-resolution spectra were collected at fixed analyzer pass energy of 160 and 20 eV, respectively. The spectra were collected at angles varying from 0° to 60° with respect to the surface normal. The binding energy (BE) values, refer to the Fermi level, and were referenced to C 1s at 284.80 eV. The standard deviation of the peak position associated with the calibration procedure was ± 0.05 eV. A commercial Kratos charge neutralizer was used to achieve a resolution of 0.6 eV

measured as a Full Width at Half Maximum (FWHM) of the P 2p peaks. The data were analyzed with commercially available software, CasaXPS (version 2313Dev64). The individual peaks were fitted by a Gaussian/Lorenzian function after linear or Shirley type background subtraction. In order to calculate the thickness and coverage, we used the high-resolution Ga 3d, P 2p, S 2p, S 2s, and C 1s spectra.

3. Results and Discussion

Very few reports have used quantitative surface characterization techniques to describe the nature of GaP substrates after chemical passivation.^{2,4,13,17} To the best of our knowledge, no prior reports have looked at a series of thiols with different end functional groups on GaP (100). We chose to use alkanethiol adsorbates because they are commercially available and have the potential to form covalent bonds with the surface. In addition, earlier efforts in this area have provided well documented evidence that sulfur containing compounds can be used in passivating strategies that result in smooth GaP surfaces with less oxide. 13 The passivation of the GaP (100) was done in solution under conditions similar to what is used to form selfassembled monolayers (SAMs) on metal and other III-V semiconductor materials. On the basis of the surface analysis we present, we discuss some notable differences and similarities among coverage, thickness, and tilt angles of short and long alkanethiols on GaP surfaces vs Au, GaAs and InP surfaces.

3.1. General Surface Characterization of Adsorbates on GaP (100) Surfaces. The native oxide layer of the GaP surface was removed by a treatment with aqua regia solution (HCl: HNO₃, 3:1, *v:v*). Freshly etched GaP surfaces were quickly placed in ethanol solution ODT, MHA, MUAM and MHL for 24 h. After this simple modification protocol preliminary studies were done using water contact angle and AFM to assess qualitatively the success of the surface functionalization.

A series of static water contact angle measurements were done on each type of surface and are summarized in Table 1. These measurements examined the homogeneity of the substrates at the microscopic level. The water contact angle for freshly cleaned GaP (100) surfaces was $19^{\circ} \pm 1$, indicating a fairly

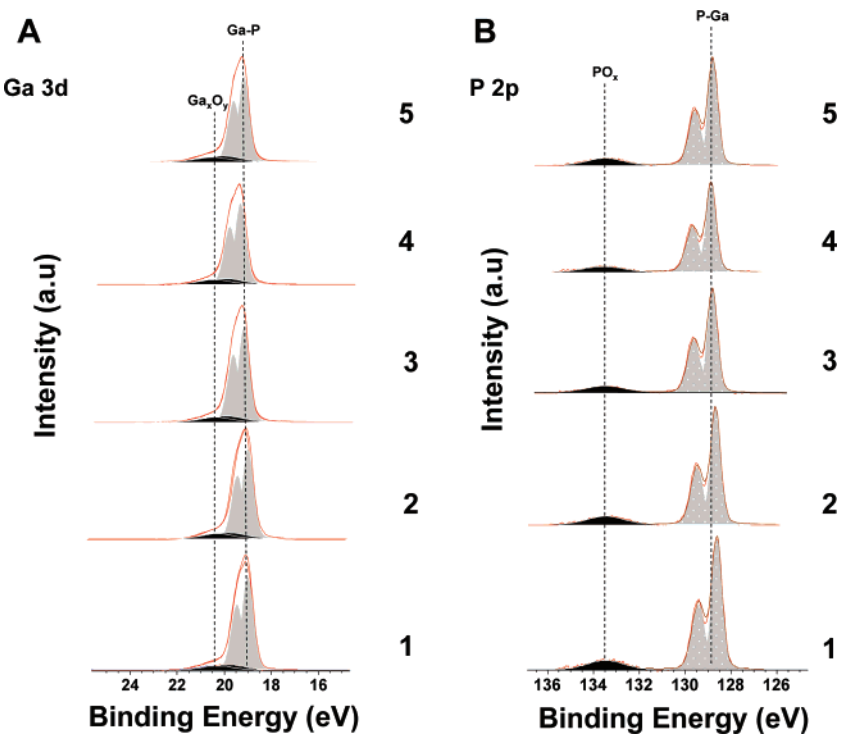


Figure 3. High-resolution XPS spectra of (A) Ga 3d and (B) P 2p for (1) clean GaP(100), (2) ODT-modified GaP(100), (3) MHA-modified GaP(100), (4) MUAM-modified GaP(100), and (5) MHL-modified GaP(100).

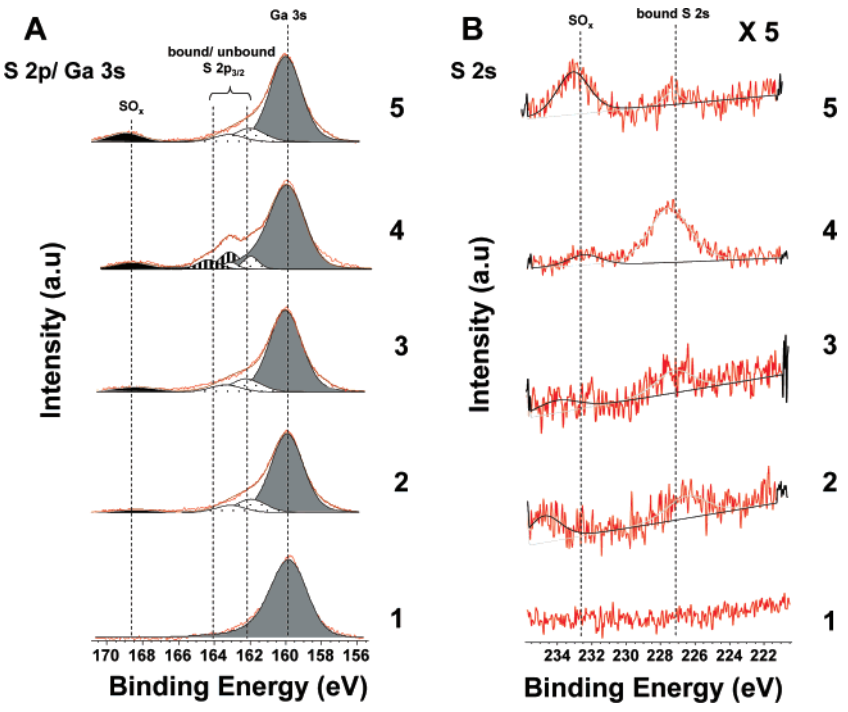


Figure 4. High-resolution XPS of (A) S 2p/Ga 3s spectra and (B) S 2s spectra for (1) freshly etched GaP(100), (2) GaP(100) functionalized with ODT, (3) GaP(100) functionalized with MHA, (4) GaP(100) functionalized with MUAM, and (5) GaP(100) functionalized with MHL.

hydrophilic surface prior to any treatment. Upon treatment with each alkanethiol, the magnitude of the contact angle increased as expected due to the nature of the end groups of the organic molecules coupled to the GaP. The hydrophobicity (φ) of the modified semiconductor surface had the following increasing order: $\varphi_{\text{Clean GaP}} < \varphi_{\text{MHL/GaP}} < \varphi_{\text{MHA/GaP}} < \varphi_{\text{MUAM/GaP}} < \varphi_{\text{ODT/GaP}}$. Our results for each of these types of adsorbates are consistent with previous surface investigations that have utilized them on various surface types. 5,6,18 High-resolution AFM scans were done in order to assess if the smoothness of the surface changed after

the passivation was done. The average root-mean-square (RMS) values are listed in Table 1. The initial roughness of the clean GaP was 0.190 ± 0.02 nm and all values measured upon passivation with the different adsorbates did not change dramatically. Overall the AFM characterization confirmed that the substrates were homogeneous in terms of their surface topography and no evidence for the formation of additional clusters on the surface was gathered after each functionalization. The angle-resolved XPS results (see below) were consistent with this conclusion. The identification of chemical species on the

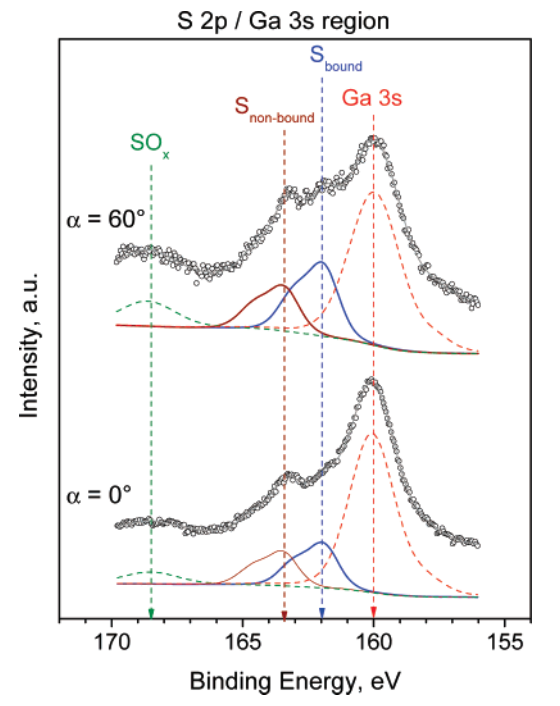


Figure 5. Deconvoluted S $2p_{3/2}$ XPS spectra for MUAM/ GaP(100) at 0° and 60° .

surface was done through two spectroscopic techniques: FT-IR and XPS.

3.2. FT-IR Characterization of the Chemical Species on GaP (100). FT-IR spectroscopy data was collected in order to prove that the adsorbates were on the surface. The data from this technique also permitted us to gather evidence for any differences in the organization of the attached molecules. The low (1550-1800 cm⁻¹) and high (2800-3000 and 3100-3800 cm⁻¹) frequency regions were examined for all types of samples and enabled us to track changes due to the presence of

TABLE 3: Summary of the Adsorption Layer Thicknesses and Tilt Angles of GaP (100) Surfaces Modified with ODT, MHA, MUAM, and MHL^a

surface	calculated thickness with Ga 3d t (Å)	calculated thickness with P 2p t (Å)	mean tilt angle (°)
A. ODT	12 ± 2	10 ± 1	63 ± 2
B. MHA	14 ± 2	9 ± 1	61 ± 4
C. MUAM	15 ± 5	11 ± 2	38 ± 5
D. MHL	8 ± 4	6 ± 4	40 ± 8

^a The values are calculated using XPS data.

alkanethiols on the GaP (100), Figure 1. We first discuss the data collected in the following regions: 1550-1800 and 3100-3800 cm⁻¹. The freshly etched GaP and ODT modified surfaces did not show any peaks (Figure 2A,B, spectra 1 and 2). After coupling of MHA and MHL to the substrate, two peaks appear at \sim 3200 and \sim 3680 cm⁻¹ and are due to the presence of -OHterminal groups (Figure 1B, spectra 3 and 5, respectively). In addition on surfaces modified by MHA adlayers a single peak at 1699 cm⁻¹ can be attributed to C=O vibrations (Figure 1A, spectrum 3).6 The appearance of amide II peaks at 1509 and 1551 cm⁻¹ was recorded on GaP modified with MUAM¹⁸ (Figure 1A, spectrum 4). Additional evidence for the presence of MUAM on the surface comes from the N-H stretching modes, Figure 1B, spectrum 4.

In our experiments, FT-IR was also used to examine the orientation and organization of the alkanethiol layers on the surfaces. The following region was examined in order to gather this information: 2800-3000 cm⁻¹. Prior to looking at the adsorbates on the GaP we collected solution FT-IR spectra for each of the adsorbates, Figure 2A, and contrasted it to data gathered on the semiconductor surfaces, Figure 2B. The position of $\nu(CH_2)$ on the spectra is used to assess if the packing of the molecules is in a liquid-like or crystalline-like state. 19-21 In the solution FT-IR spectra, the symmetric and asymmetric stretching

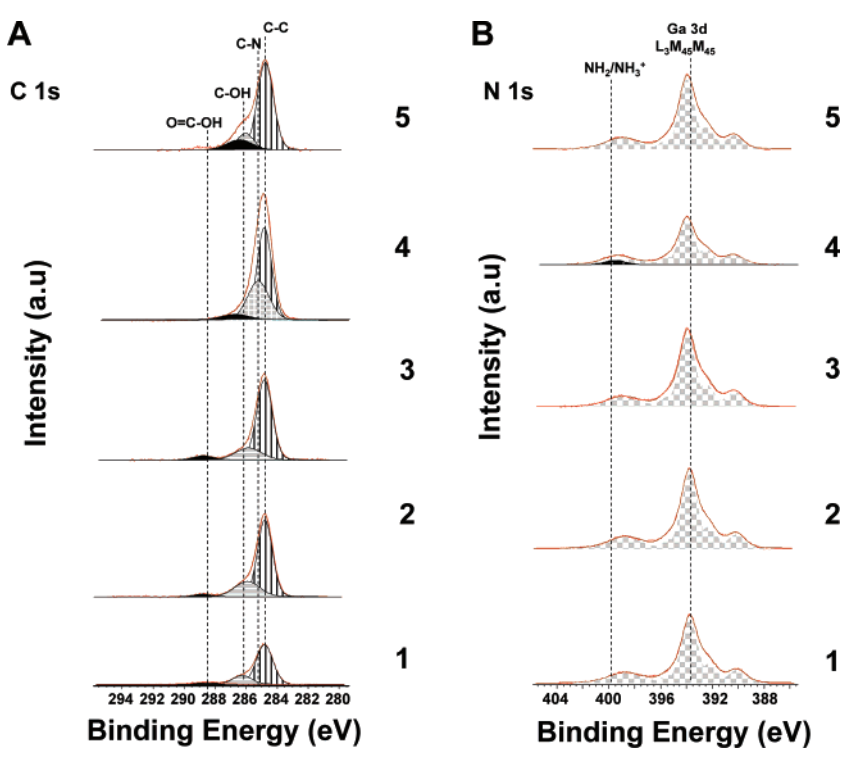


Figure 6. High-resolution XPS spectra in the region corresponding to (A) C 1s and (B) N 1s for (1) clean GaP, (2) ODT assembled on GaP(100), (3) MHA assembled on GaP(100), (4) MUAM assembled on GaP(100), and (5) MHL assembled on GaP(100).

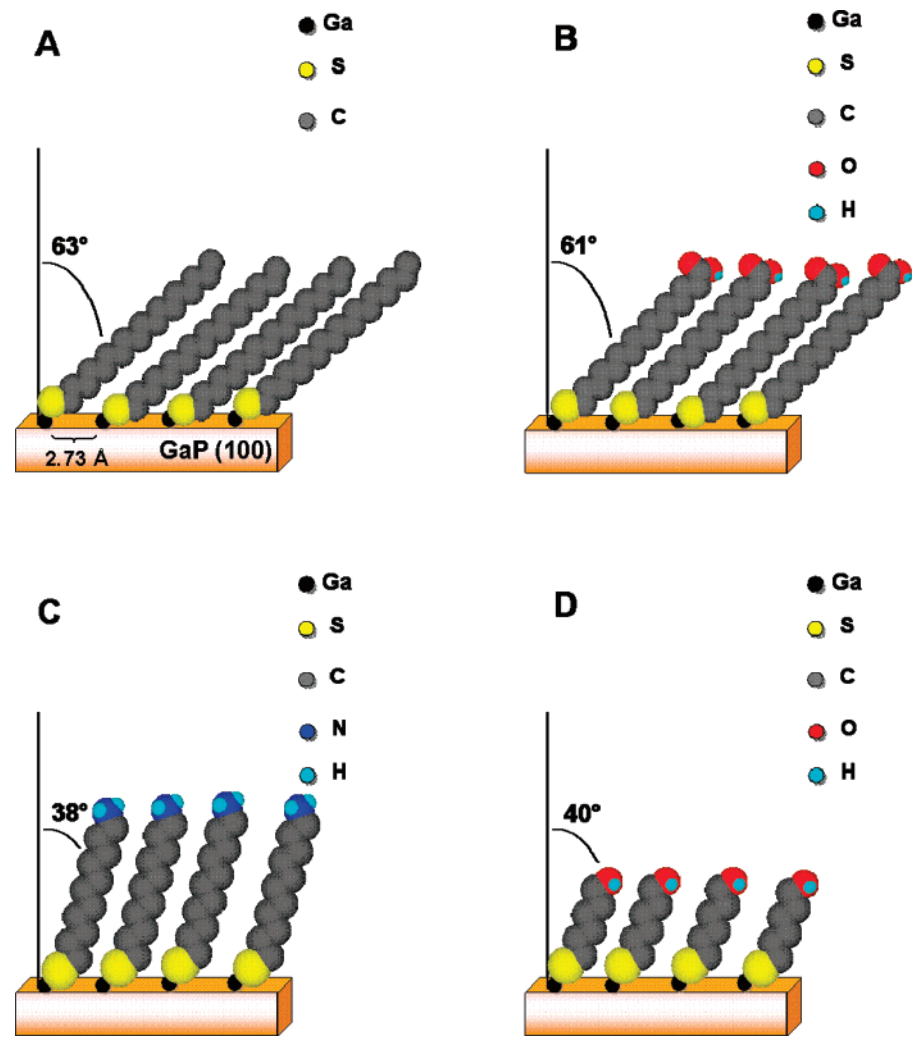


Figure 7. Schematic representation of the orientation of each adsorbate on GaP (100): (A) ODT, (B) MHA, (C) MUAM, and (D) MHL.

mode of $\nu(\text{CH}_2)$ were positioned at $\sim\!2851\!-\!2855$ and 2924–2931 cm⁻¹, respectively. After the absorption of the alkanethiol molecules on GaP, the asymmetric/ symmetric $\nu(\text{CH}_2)$ bands were recorded at 2918 cm⁻¹/2850 cm⁻¹, 2922 cm⁻¹/2852 cm⁻¹, 2919 cm⁻¹/2849 cm⁻¹, and 2920 cm⁻¹/2847 cm⁻¹ for ODT, MHA, MUAM, and MHL, respectively. This data supports the notion that the molecules are in a crystalline-like state on the GaP surface since the vibrational frequencies were 2–5 cm⁻¹/2–3 cm⁻¹ lower for asymmetric/symmetric $\nu(\text{CH}_2)$. In summary, the FT-IR data confirmed the presence of the adsorbates on the surface but did not allow us to understand if there are differences in the mode of attachment to the surface among the four alkanethiols. XPS data was collected in order to address this important question.

3.3. X-ray Photoelectron Spectroscopy. XPS is a powerful technique, which provides quantitative and qualitative data with regard to the chemical composition of the adsorption layer. We investigated each type of surface modification by XPS. The analysis was based on the core level spectra of gallium, phosphorus, sulfur, carbon, nitrogen and oxygen, namely Ga 3d and Ga 2p, P 2p, S 2p and S 2s, C 1s, N 1s, and O 1s. In order to extract complete information from the peak shape, the spectra were fitted assuming a Gaussian/Lorenzian line shape. The curve fitting is particularly important for the N 1s and S 2p analysis because these photoelectron transitions overlap with the Ga Auger and Ga 3s peaks, respectively. The peak positions for clean and modified GaP(100) are summarized in Table 2 and were obtained after curve-fitting. As shown in Figure 3,

after cleaning the GaP(100) still demonstrated the Ga 3d peaks at \sim 21 eV, which is the characteristic of Ga_xO_y.6One can also observe the P 2p peak at \sim 134 eV, which is typical for P_xO_y.5 The oxidation likely happens when the samples are exposed to air during their transfer to the XPS instrument. All samples that we examined after the adsorption of ODT, MHA, MUAM, and MHL layer showed a decreased amount of oxide. No specific components corresponding to a phosphorus-sulfur bond and a gallium-sulfur bond could be resolved in the Ga 3d and P 2p spectra.

Figure 4 represents the S 2p/Ga 3s and S 2s core level spectra. The S 2s spectra were acquired to validate our curvefitting procedure, which is critical for the extraction of the S 2p contribution. For clean GaP, the Ga 3s peak is asymmetric and set at 160.5 eV (see dark gray peak in Figure 4). After the immobilization of the alkanethiols on the surface, the sulfur peaks became detectable. The S 2p doublet, exhibiting a 1.15 eV separation, is plotted as white/dotted peaks in Figure 4A, and is at ca. 162 eV. This BE is characteristic for covalently bond sulfur to the substrate. 3-8,13,23 Oxidized sulfur manifests itself with a high BE peak at ~169 eV.3,5,7,23 In the case of the MUAM/GaP(100) surface, an additional component is detected at 163.2 eV. Figure 5A shows the S 2p spectra obtained from MUAM/GaP(100) at 0 and 60° collection angles with respect to the surface normal. Two distinct S 2p components were assigned to the sulfur atoms covalently bound to the surface (162 eV for S 2p_{3/2}) and to sulfur that is not bonded to the surface 23,24 (163.2 eV for S $2p_{3/2}$). As shown in Figure 5,

TABLE 4: Summary of Alkanethiol Coverages (ML) Using S 2p, S 2s, C 1s, Ga 3d, and P 2p XPS Intensities from Surfaces Modified with ODT, MHA, MUAM, and MHL

	coverage, Θ (ML)					
surface	$\Theta_{S2p/Ga3d}$ (molecules/nm ²)	$\Theta_{S2s/Ga3d} $ (molecules/nm ²)	$\Theta_{C1s/Ga3d}$ (molecules/nm ²)	$\Theta_{S2p/P2p}$ (molecules/nm ²)	$\Theta_{S2s/P2p}$ (molecules/nm ²)	Θ _{C1s/P2p} (molecules/nm ²)
A.ODT	0.80 ± 0.2 (10 ± 5)	0.30 ± 0.08 (4 ± 2)	0.39 ± 0.03 (5 ± 2)	0.84 ± 0.2 (12 ± 3)	0.31 ± 0.08 (4 ± 1)	0.41 ± 0.02 (6 ± 1)
B.MHA	0.86 ± 0.3 (10 ± 3)	0.32 ± 0.05 (4 ± 3)	0.44 ± 0.1 (6 ± 2)	0.89 ± 0.3 (11 ± 4)	0.33 ± 0.05 (4 ± 1)	0.41 ± 0.1 (6 ± 1)
C.MUAM	0.94 ± 0.2 (13 ± 3)	1.1 ± 0.1 (16 ± 1)	1.2 ± 0.03 (17 ± 10)	0.99 ± 0.3 (13 ± 4)	1.2 ± 0.08 (16 ± 1)	1.2 ± 0.03 (11 ± 7)
D.MHL	0.89 ± 0.2 (12 ± 2)	0.47 ± 0.1 (7 ± 3)	0.20 ± 0.05 (3 ± 2)	0.98 ± 0.2 (13 ± 3)	0.52 ± 0.1 (8 ± 2)	0.22 ± 0.03 (2 ± 1)

the emission angle variation does not lead to change in the ratio between the two sulfur forms at 162 and 163.2 eV. The ratio between this component and the Ga 3s peak also changes proportionally with the emission angle. This allows us to draw the conclusion that the two sulfur states occupy similar positions on the surface. Surprisingly, the nonbond state is as close to the surface as the bond one. Two possible explanations can be proposed. First, the MUAM molecules can couple through the amine group. But in this case, the coupled MUAM likely bends over the amine group center and the second end of the molecule points down. It is unlikely that the coupled MUAM molecules would be pointing straight up because this scenario will contradict (i) the photoemission angle dependence and (ii) the calculated thickness of the adlayer described below. Another explanation could be an "up-side-down" configuration, in which approximately half of the MUAM molecules bind to the surface through the amine group. In this case the amine group, which is an electron donor, can stabilize adjacent MUAM molecules adsorbed through sulfur. Unfortunately, the N 1s region is crowded with the Ga Auger and we could not distinguish two different nitrogen states. Therefore it is difficult to state which of the two explanations is more likely to be happening.

In order to perform more reliable data quantification, the S 2s region was also acquired from the GaP(100) surfaces functionalized with ODT, MHA, MUAM, and MHL (Figure 4B). Two peaks were detected in the S 2s spectra. The first peak at ~227 eV is characteristic of thiol groups, whereas the second peak at ~232.5 eV originates from oxidized sulfur.

The C 1s and N 1s spectra are shown in Figure 6, panels A and B, respectively. The cleaned GaP (100) surface showed carbon contaminations due to the sample exposure to air. A notable increase of the C 1s peak intensity was observed for all GaP substrates modified with alkanethiols compared to the cleaned surface. For surfaces modified with MHA and MHL, components corresponding to OH-C=O and C-OH were detected at 288.8 and 286.0 eV, respectively. The MUAM adlayer on the GaP(100) surface showed a C 1s component at 286.6 eV. The N 1s peak was centered at 399.5 eV and can be assigned to C-N and NH₂/NH₃⁺ species. It should be noted that the N 1s peak was extracted using curve fitting. As shown in Figure 6B, the Ga L₃M₄₅M₄₅ auger lines²⁵ were observed for clean GaP(100), ODT/GaP(100), MHA/GaP(100), MUAM/ GaP(100), and MHL/GaP(100). The Auger line shape was extracted from the spectra obtained from the clean surface and then the Auger line constraint was used to deconvolute the N 1s peak.

As stated above XPS can supply quantitative and qualitative data. In this study we utilized the XPS data to calculate the adlayers thicknesses and the tilt angles of the adsorbed molecules on the GaP(100) surface. In order to increase the accuracy, first, we collected the electron emission at different angles, α , varying

from 0° to 75° in respect to the surface normal. Subsequently, the Ga 3d and P 2p peaks were used for the calculations. The adlayer thickness was calculated using the attenuation of the core level peaks of the substrate (in our case it was Ga 3d and P 2p) as given by the equation

$$I = I^0 \left(1 - \frac{-t}{e^{L \cdot \cos \alpha}} \right) \tag{1}$$

where I^0 and I are the intensities of the Ga 3d and P 2p peaks obtained from the clean GaP surface and after the alkanethiol immobilization, respectively. The clean GaP surface was prepared by short Ar⁺ sputtering of the sample that was cleaned with aqua. The thickness is defined as t in Å. L is the electron attenuation length (EAL), which was used instead of the inelastic mean free pass (IMFP) of the photoelectrons as suggested by Jablonski and Powell.²⁶ The EAL values for the Ga 3d and P 2p photoelectrons were calculated using the NIST SRD- 82 software.²⁷ The EAL values and the parameters needed for these calculations are summarized in the Supporting Information, Table S-2. The mean thickness and mean tilt angle values are summarized in Table 3. The mean thickness was calculated by plotting $ln(I/I^0)$ versus $1/cos(\alpha)$ and the slope of the resulting line is equal to -t/L. The advantage of this approach is that the line of $ln(I/I^0)$ versus $1/cos(\alpha)$ was drawn with the least-square method. Therefore, this protocol gives more precise results compared to values obtained from single angle measurements. The tilt angles were calculated using the adlayer thicknesses and assuming the molecule lengths of ODT, MHA, MUAM, and MHL to be 24.0, 22.5, 16.7, and 9.84 Å, respectively.

The thickness of the ODT adlayer is in good agreement with previous works on GaAs. ^{23,28–30} As shown in Table 3 and Figure 7, the tilt angles were slightly different from the ones obtained with alkanethiol species on GaP (110), Au (100), and Ag (111) surfaces.^{2,31} However, our values were similar to those for thiolate-SAMs on GaAs (100), InP (100), and Au (111) substrates.5,6,23,31 According to our data, ODT and MHA molecules have higher tilt angles compared to MUAM and MHL.

In order to confirm the quality of the adsorption layer, the adsorbate coverage was calculated for each modified surface using the intensities of S 2p, S 2s, C 1s, Ga 3d, and P 2p. We applied the approximation method for a semi-infinite substrate with a non-attenuating overlayer, ^{32,33} which is described by the following equation:

$$\frac{N_{\rm l}(\alpha)}{N_{\rm k}(\alpha)} = \frac{\Omega_0 E_{\rm l} A_0(E_{\rm l}) D_0(E_{\rm l}) \frac{{\rm d}\sigma_{\rm l}}{{\rm d}\Omega} {\rm d}}{\Omega_0 E_{\rm k} A_0(E_{\rm k}) D_0(E_{\rm k}) \frac{{\rm d}\sigma_{\rm k}}{{\rm d}\Omega} \Lambda_{\rm e}^{\rm subst}(E_{\rm k}) \cos\alpha} \begin{pmatrix} s_{\rm overl} \\ s_{\rm subst} \end{pmatrix} \quad (2)$$

where $N_l(\alpha)$ and $N_k(\alpha)$ are the peak areas of the molecular adlayer and the substrate at the given emission angle, α , respectively; Ω_0 is the acceptance solid angle of the electron analyzer; A_0 and D_0 are the effective area of the specimen and the instrument detection efficiency, respectively; $d\sigma_{(k \text{ or })}/d\Omega$ is the tabulated differential cross-section from the Scofield crosssections³⁴ including a correction for the Reilman asymmetric parameter; $\Lambda_e^{\text{subst}}(E_k)$ is the IMFP of the photoelectron in the substrates; α is the angle between the surface normal and the electron emission direction; soverl/ssubst is the fractional monolayer coverage of the atomic species where s_{overl} and s_{subst} are the mean surface density of atoms and the mean surface density of substrate atoms in cm^{-2} , respectively; and d is the mean separation between layers of density s in the substrate, which for GaP (100) is 2.73 Å. After some terms cancellation, eq 2 can be modified to

$$\Theta = \frac{N_l}{N_k} \frac{\frac{d\sigma_k}{d\Omega} \Lambda_e^{GaP}(E_k) \cos\alpha}{\frac{d\sigma_l}{d\Omega} d}$$
(3)

where the coverage (Θ) is measured in monolayer, ML; N_k represents the intensity of the Ga 3d or P 2p peaks; N_l is the intensity of the S 2p or S 2s or C 1s peaks. $\Lambda_e^{\text{GaP}}(E_k)$ can be substituted with the average EAL for gallium phosphide calculated by NIST SRD-82 (Table S-2 in the Supporting Information). The calculated coverages in ML and molecules/nm² are shown in Table 4. Monolayer (ML) is the ratio between surface concentration of adsorbed molecules and the number of surface atoms per unit of area. The number of gallium atoms on the non-reconstructed GaP(100) surface is assumed to be 1.36×10^{15} at/cm². The coverages were also calculated by the approach validated by Popat et al. for and Petrovykh et al., for and the values obtained are presented in the Supporting Information. The discussion below is based on calculations using eq 3.

The calculated coverages using the S 2s, C 1s, Ga 3d, and P 2p intensities are fairly consistent. However, the results obtained using the S 2p intensities are not in good agreement with the other values. The discrepancy can arise from uncertainty in determining the S 2p contribution. As it was mentioned above the Ga 3s peak overlaps with S 2p. This is not symmetric and hinders the extraction of the precise contribution of S 2p at low coverage of the adsorbed layer. This problem does not exist for monolayer coverage, e.g., MUAM/ GaP(100), where all calculations yielded consistent coverage values. We also encountered this problem for the same thiols on GaAs.³⁷ The maximum and minimum molecular well-packing were obtained on MUAM/GaP (~1.2 ML/17 molecules/nm²) and MHL/GaP (0.22 ML/ 2 molecules/nm²).

Figure 7 compares the arrangement of the different alkanethiols on this surface. Desptie the high tilt angle values for ODT and MHA, all adsorbates passivated the GaP (100) surface well and prevented the re-formation of oxide on the surface. Our alkanethiol adsorption layer on GaP(100) showed higher coverages compared to thiolate species on Au (4.5 molecules/nm²)³⁸ and InP (~1 molecules/nm²).⁵ Our results show that even alkanethiols with reactive head groups can sufficiently passivate the surface. Our data re-confirm previous reports that solution modification of GaP with alkanethiols can be offer defined orientation of the molecules on the surface.² Therefore in future efforts we plan to apply the alkanethiol passivation protocol and characterization methodology to devices containing active layers of GaP.

4. Conclusions

This study reports the complete and quantitative characterization of alkanethiol adsorption layers on GaP(100) surfaces. The presence of characteristic functional groups for each adlayer was confirmed via FT-IR spectroscopy and wettability experiments. The thickness values and AFM data confirmed the formation of the smooth layers of thiolate species on the GaP-(100) surface. Each surface was characterized by quantitative XPS measurements. The XPS data was utilized to calculate the thickness, tilt angles and coverage values. The quantitative information we report contributes to the understanding of the properties of organized layers of III—V semiconductor surfaces. This type of information can be used in the functionalization of devices such as light emitting diodes.

Acknowledgment. This work was supported by NSF under CHE-0614132.

Supporting Information Available: Additional data analysis of the XPS spectra presented in the manuscript. This material is available free of charge via the Internet at http://pubs.acs.org.

References and Notes

- (1) Sheen, C. W.; Shi, J.-X.; Martensson, J.; Patrick, A. N.; Allara, D. L. J. Am. Chem. Soc. **1992**, 114, 1514—1515.
- (2) Chasse, T.; Zerulla, D.; Hallmeier, K. H. Surf. Rev. Lett. 1999, 6, 1179–1186.
- (3) McGuiness, C. L.; Shaporenko, A.; Mars, C. K.; Uppili, S.; Zharnikov, M.; Allara, D. L. *J. Am. Chem. Soc.* **2006**, *128*, 5231–5242.
- (4) Liu, K. Z.; Suzuki, Y.; Fukuda, Y. Surf. Interface Anal. **2004**, *36*, 966–968.
- (5) Park, H. H.; Ivanisevic, A. J. Phys. Chem. C 2007, 111, 3710-3718.
 - (6) Cho, Y.; Ivanisevic, A. J. Phys. Chem. B 2005, 109, 12731–12737.
- (7) McGuiness, C. L.; Shaporenko, A.; Zharnikov, M.; Walker, A. V.; Allara, D. L. J. Phys. Chem. C 2007, 111, 4226–4234.
- (8) Yang, G. H.; Zhang, Y.; Kang, E. T.; Neoh, K. G.; Huang, W.; Teng, J. H. *J. Phys. Chem. B* **2003**, *107*, 8592–8598.
- (9) McGuiness, C. L.; Blasini, D.; Masejewski, J. P.; Uppili, S.; Cabarcos, O. M.; Smilgies, D.; Allara, D. L. ACS Nano 2007, I, 30–49. (10) Wang, Y.; Ramdani, J.; He, Y.; Bedair, S. M.; Copper, J. A.; Melloch, M. R. IEEE Electron. Device Lett. 1993, 29, 1154–1156.
 - (11) Woodall, J. Science 1977, 196, 990-991.
- (12) Beck, A. L.; Yang, B.; Wang, S.; Collins, C. J.; Campbell, J. C.; Yulius, A.; Chen, A.; Woodall, J. M. *IEEE J. Quantum Electron.* **2004**, 40, 1695–1699.
- (13) Suzuki, Y.; Sanada, N.; Shimomura, M.; Fukuda, Y. Appl. Surf. Sci. 2004, 235, 260–266.
 - (14) Ismail, M. S.; Bowler, R. W. Electron. Lett. 1991, 27, 1153-1155.
- (15) Chen, A.; Woodall, J. M. Appl. Phys. Lett. 2007, 90, 103509-1-3.
- (16) Popat, K. C.; Swan, E. E. L.; Desai, T. A. Langmuir 2005, 21, 7061–7065.
 - (17) Lu, Z. H.; Graham, M. J. J. Appl. Phys. 1994, 75, 7567-7569.
- (18) Flores-Perez, R.; Ivanisevic, A. Appl. Surf. Sci. 2007, 253, 4176–4181.
- (19) Nuzzo, R. G.; Dubois, L. H.; Allara, D. L. J. Am. Chem. Soc. 1990, 112, 558–569.
- (20) Li, Z.; Chang, S. C.; Williams, R. S. Langmuir **2003**, *19*, 6744–6749.
- (21) Nakano, K.; Sato, T.; Tazaki, M.; Takagi, M. Langmuir **2000**, *16*, 2225–2229.
- (22) Lee, C. Y.; Harbers, G. M.; Grainger, D. W.; Gamble, L. J.; Castner, D. G. *J. Am. Chem. Soc.* **2007**, *129*, 9429–9438.
- (23) Jun, Y.; Zhu, X.-Y.; Hsu, J. W. P. Langmuir 2006, 22, 3627–3632.
- (24) Uvdal, K.; Vikinge, T. P. Langmuir 2001, 17, 2008-2012.
- (25) Staib, P.; Contour, J. P.; Massies, J. J. Vacuum Sci. Technol. A 1985, 3, 1965–1968.
 - (26) Jablonski, A.; Powell, C. J. Surf. Sci. Rep. 2002, 47, 33-91.
- (27) Powell, C. J.; Jablonski, A. *NIST Electron Effective- Attenuation-Length Database*, *Version 1.0 SRD-82*); Department of Commerce; National Institute of Standards and Technology: Gaithersburg, MD, 2001.
- (28) Ye, S.; Li, G.; Noda, H.; Uosaki, K.; Osawa, M. Surf. Sci. 2003, 529, 163–170.

- (29) Zhang, Q.; Huang, H.; He, H.; Chen, H.; Shao, H.; Liu, Z. Surf. Sci. **1999**, 440, 142-150.
 - (30) Baum, T.; Ye, S.; Uosaki, K. Langmuir 1999, 15, 8577-8579.
- (31) Yamamoto, H.; Waldeck, D. H. J. Phys. Chem. B **2002**, 106, 7469–7473.
- (32) Jedlicka, S. S.; Rickus, J. L.; Zemlyanov, D. Y. *J. Phys. Chem.* **2007**, *111*, 11850–11857.
- (33) Fadley, C. S. Basic concepts of x-ray photoelectron spectroscopy 1978; Vol. 2.
- (34) Scofield, J. H. J. Electron Spectrosc. Relat. Phenom. 1976, 8, 129–137.
- (35) NIST Electron Effective-Attenuation-Length Database, SRD-82, version 1.1; National Institute of Standards and Technology: Gaitherburg, MD, 2003.
- (36) Petrovykh, D. Y.; Kimura-Suda, H.; Tarlov, M. J.; Whitman, L. J. *Langmuir* **2004**, *20*, 429–440.
- (37) Lee, K.; Wampler, H. P.; Nair, P. R.; Zemlyanov, D. Y.; Alam, M. A.; Janes, D. B.; Ivanisevic, A. *J. Appl. Phys.* **2007**, submitted.
- (38) Heister, K.; Frey, S.; Golzhauser, A.; Ulman, A.; Zharnikov, M. J. J. Phys. Chem. B **1999**, 103, 11098–11104.